J Electr Eng Technol.2017; 12(6): 2106-2117
http://doi.org/10.5370/JEET.2017.12.6.2106

ISSN(Print) 1975-0102
ISSN(Online) 2093-7423

Fault Location and Classification of Combined Transmission System: Economical and Accurate Statistic Programming Framework

J. Tavalaei*, M. H. Habibuddin†, A. Khairuddin* and A. A. Mohd Zin*

Abstract – An effective statistical feature extraction approach of data sampling of fault in the combined transmission system is presented in this paper. The proposed algorithm leads to high accuracy at minimum cost to predict fault location and fault type classification. This algorithm requires impedance measurement data from one end of the transmission line. Modal decomposition is used to extract positive sequence impedance. Then, the fault signal is decomposed by using discrete wavelet transform. Statistical sampling is used to extract appropriate fault features as benchmark of decomposed signal to train classifier. Support Vector Machine (SVM) is used to illustrate the performance of statistical sampling performance. The overall time of sampling is not exceeding 1¼ cycles, taking into account the interval time. The proposed method takes two steps of sampling. The first step takes ¾ cycle of during-fault and the second step takes ¼ cycle of post fault impedance. The interval time between the two steps is assumed to be ¼ cycle. Extensive studies using MATLAB software show accurate fault location estimation and fault type classification of the proposed method. The classifier result is presented and compared with well-established travelling wave methods and the performance of the algorithms are analyzed and discussed.

Keywords: Fault location, Combined transmission line, Wavelet transform, SVM, Feature extraction

1. Introduction

High voltage Transmission Line (TL) is designed based on the maximum power required at the receiving end and the related voltage. Normally, Over-Head Line (OHL) is constructed by a similar conductor with homogenous characteristics to avoid any stress on non-homogeneous sections. However, in several cases, such as electrification of islands, offshore regions and long span OHL, a designer may connect OHL with an Under-Ground Cable (UGC). Moreover, junctions can be added to OHL in order to feed newly constructed TL or connect the upstream network to a microgrid [1-3]. These issues will change the homogeneity of line characteristics.

Fault detection and classification methods [4, 5] (fault analysis) are divided into impedance measurement and Travelling Wave (TW) methods. In TW theory, high frequency waves generated during the fault on a transmission line are studied. These high frequency signals can be extracted by using an advanced signal processing technique [6].

These high frequency waves travelled toward both ends of the transmission line. They will be reflected when the waves face discontinuity. Therefore, the fault location can be estimated by using TW equations [7]. The implementation of TW method is more expensive compared to impedance-based method due to the requirements for high frequency data acquisition system and a highly accurate common time reference at both ends [8]. On the other hand, measured impedance in a TL is proportional to line length and is derived from Ohm's Law. The impedance measurement method [9] is not a costly method but rather is affected by fault resistance.

The electrical characteristics of OHL and UGC for the same voltage level are quite different. This issue affects the measurement and monitoring devices of combined TL significantly. Combined TL is affected by two major issues: non-homogeneous characteristics of TL and charging current in UGC. A large charging current of UGC affects the impedance measurement method. When the fault occurred on the cable section, the measured impedance is changed due to current variation, cable cross bounding, grounding method, etc. Hence, fault detection methods are applied on UGC faced with mis-operation [10]. Although the combined transmission is a special scheme for protection, the interesting characteristics of the combined section are valuable for the study. The power system is mainly protected by algorithmic-based protection [6, 7, 11-14]. These techniques are more useful when the network suffers from non-homogenous impedance of combined transmission line. The proposed method is validated on a modified combined transmission system [15]. This study is providing further development on combined transmission line fault location estimation and

† Corresponding Author: Department of Electrical Power Engineering, Universiti Teknologi Malaysia (UTM), Malaysia. (mhafiz@fke.utm.my)
* Department of Electrical Power Engineering, Universiti Teknologi Malaysia (UTM), Malaysia. (jalal.tavalaei@fkegraduate.utm.my, azharkhairuddin@utm.my, asuhaimi@utm.my)
Received: January 12, 2016; Accepted: June 26, 2017

Copyright ⓒ The Korean Institute of Electrical Engineers
This is an Open-Access article distributed under the terms of the Creative Commons Attribution Non-Commercial License (http://creativecommons.org/licenses/by-nc/3.0/) which permits unrestricted non-commercial use, distribution, and reproduction in any medium, provided the original work is properly cited.

fault type classification based on the proposed statistical sampling. Normally, the fault analysis for combined TL is fulfilled by TW without considering the cost. Then the main contribution of this paper is taking into account the fault location estimation and fault type classification accuracy as well as cost. Support Vector Machine (SVM) is used for classification because it is less likely to over-fit and new sample data can be added to system due to shorter time of training compared with Artificial Neural Network (ANN) [11]. To achieve this aim, an impedance-based single-ended method is developed to reach fault analysis in minimum cost. The Proposed Method (PM) is an online system which can be used in offline analysis. Finally, the PM is compared with double-ended TW [15] and single-ended [16] techniques for a comprehensive analysis.

2. Economic Analysis

This research is taking into account the fault location estimation and fault type classification accuracy as well as cost. The economic analysis considers cost of installation and maintenance as well as time of operation and accuracy on fault detection and estimation.

2.1 Cost analysis

The estimated cost of proposed method and TW method is tabulated in Table 1 for the most important equipment. It illustrates that installation of double-ended TW and single-ended TW methods are around 100,000.00 USD and 40,000.00 USD more than PM, respectively. On the other hand, the number of equipment used in TW methods are more than PM. Therefore, the total cost of PM is much less than TW methods, taking into account the maintenance and repair services costs. TW methods accuracy is improved by using optical transducer; thereby the installation price is going to increase by including optical equipment [16].

2.2 Time of operation

The PM uses 1¼ cycles of fault data, which is faster than high speed protective relays [17]. In other words, the circuit breaker will open the TL in 1¼ cycles. The consumed time for feature extraction is 3 milliseconds and time of SVM operation is around 1.5 milliseconds, with a core i3 processor and 8 GB RAM. Therefore, the overall time for a fault analysis does not exceed 30 milliseconds and can be further reduced by using a higher performance computer. The sampling rate for PM is 11.52 kHz [18].

The time of fast fault detection for TW method is few milliseconds and the overall operation time for detecting the fault location for TW method is in a matter of seconds with sampling rate of 36 MHz [19].

Table 1. The estimated cost of methods

Method	PM (USD)	TW (USD)	
		Single-ended	Double-ended
CT	3×7,500.0	3×7,500.0	6×7,500.0
CVT	3×8,000.0	3×10,000.0	6×10,000.0
Computer	500.0	500.0	500.0
TR	15,500.0	3×17,250.0	3×17,250.0
GPS	-	-	3×2,500.0
Total	62,500.0	104,750.0	164,750.0

CT: Current Transformer, CVT: Capacitive Voltage Transformer, TR: Transient Recorder, GPS: Global Positioning System.

2.3 Accuracy analysis

The worst case of fault is reported for a fault with simultaneous high resistance and small inception angle [15, 16]. The accuracy analysis is 0.21 km, 3.8 km and 2.0 km on combined transmission line for double-ended TW [15], single-ended TW [16] and PM, respectively. The accuracy of double-ended TW is a critical issue when the remote connection is missed [19]. These comparisons are tabulated in sections 7 and 8.

3. System Model

OHL and UGC are modeled in order to obtain high accuracy. The simulated system is tested under typical fault types. Fig. 1 presents the flowchart of fault feature extraction in combined TL.

The positive sequence impedance is extracted after modal decomposition on waveforms. Then, wavelet transform is implemented on the measured impedance signal. The decomposed signal is statistically sampled to find the signal features. Finally, extracted features are used as a benchmark of fault signal to develop the fault analysis procedure. These features are used to train SVM classifier to estimate fault location and cluster fault type.

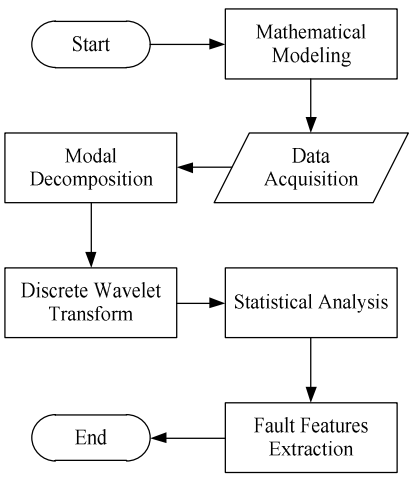

Fig. 1. Flowchart of fault feature extraction

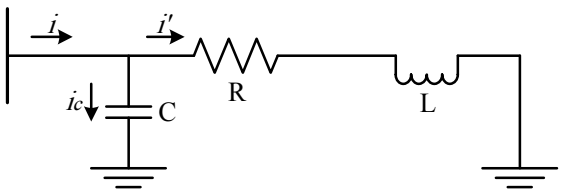

Fig. 2. Modeling of charging current for cable section

3.1. Mathematical modeling

To mathematically model the combined transmission system, the cable section needs to be analysed adequately [20, 21]. The equivalent lumped parameter model for cable section is represented in Appendix A. The main problem of cable is the huge rate of charging current. The cable section of combined transmission line is modelled in Fig. 2.

The i_c and i represent capacitive current and cable current, respectively. The charging current compensation based on presented model [22] is improved for equivalent lumped parameter model.

$$V = Ri' + L\frac{di'}{dt} \tag{1}$$

$$i' = i - i_c = i - Y/2\frac{dV}{dt} \tag{2}$$

The term *Y/2* in (2) represents half of the total capacitance of cable [22]. Now, by using two times integration of (1) and (2):

$$\int_{t-T}^{t}\int_{t-T}^{t} Vdt^2 = R\int_{t-T}^{t}\int_{t-T}^{t} i'dt^2 + L\int_{t\_T}^{t} i'dt \tag{3}$$

$$\int_{t-T}^{t} i'dt = \int_{t-T}^{t} idt - Y/2V \tag{4}$$

$$\int_{t-T}^{t}\int_{t-T}^{t} i'dt^2 = \int_{t-T}^{t}\int_{t-T}^{t} idt^2 - Y/2\int_{t-T}^{t} Vdt \tag{5}$$

and by substituting (4) and (5) in (3):

$$\begin{aligned}\int_{t-T}^{t}\int_{t-T}^{t} Vdt^2 &= R\left[\int_{t-T}^{t}\int_{t-T}^{t} idt^2 - Y/2\int_{t-T}^{t} Vdt\right] \\ &+L\left[\int_{t-T}^{t} idt - Y/2V\right]\end{aligned} \tag{6}$$

Now, by substituting the terms of equivalent lumped parameter into (6), the equation is as follows:

$$\int_{t-T}^{t}\int_{t-T}^{t} Vdt^2 = Rl\frac{\sinh\gamma l}{\gamma l}\left[\int_{t-T}^{t}\int_{t-T}^{t} idt^2 - Y/2\frac{\tanh(\gamma l/2)}{\gamma l/2}\int_{t-T}^{t} Vdt\right]$$

$$+Ll\left[\int_{t-T}^{t} idt - Y/2\frac{\tanh(\gamma l/2)}{\gamma l/2}V\right] \tag{7}$$

The (7) covers the non-homogeneity and charging current compensation simultaneously.

Fig. 3 illustrates the combined transmission line analysis after fault is executed. The 'Z_{TL}' represents the total equivalent transmission line impedance, 'Z_s' and 'p' are the source impedance and fault position, respectively. The detailed parameters of combined transmission line are presented in Appendix B.

The analysis of charging current and non-uniform conductors are combined and solved for the impedance measurement at relay point.

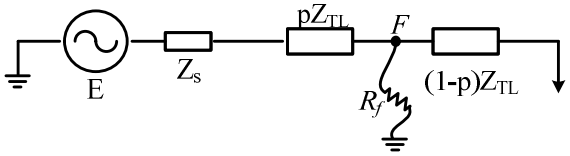

Fig. 3. Single diagram of fault analysis on combined TL

3.2. Modal decomposition

After transformation of the voltage and current to sequence components, the positive sequence impedance (Z^{pos}) is calculated from Ohm's Law to be used in fault analysis. It is useful to extract features of signal for protective purposes. This signal covers three phase components to reduce time of analysis and calculation burden. The overall time of sampling is not exceeding 1¼ cycles taking into account the interval time. The proposed method takes two steps of sampling. In the first step, it takes ¾ cycle and in the second step, takes ¼ cycle of fault impedance. The interval time between the two steps is ¼ cycle.

3.3. Wavelet transform

In the protection scheme, time of signal processing is vital. Therefore, Discrete Wavelet Transform (DWT) is applied to the signal. The DWT is used as a variable data window at fault time to increase the resolution of the detail signal [11, 23]. This is because the resolution depends on time and fault signal value. The impedance waveform is carrying high frequency signals which are generated with respect to fault location, fault resistance, fault angle and fault type. Extracted coefficients of approximation and detail of DWT are used as a benchmark for fault analysis. When the wavelet transform is implemented on a signal, the most important issue is to choose the best level of analysis and data window length. A higher decomposition level will increase the resolution of time-frequency scaling, but the valuable part of the signal in high frequencies is

missed. When the scaling and translation increase, the high frequency signals are faded. These high frequency signals carry the important features of fault signal. A fault signal will be decomposed to approximation and detail signals by appropriate mother wavelet.

4. Feature Extraction and Machine Learning

Support vector machine was used for classification problems in statistical learning theory and structural risk minimization. It uses structural minimization principles to choose discriminative function that have minimal risk bound; the necessary training sample size is smaller. Hence, SVMs are less likely to over-fit data than over classification algorithm such as ANN [11].

4.1. Support Vector Machine (SVM)

The SVM attitude shows more systematic approach to learn linear and non-linear decision boundaries. Although the SVMs are usually used to fault classification on transmission lines, they can be applied for fault location estimation [24].

The SVM classifier finds an optimal hyperplane to separate data sets with different classes ({+1, −1}). The linear hyperplane is defined by a weight vector W and a term b as [16]:

$$W^T x + b = \begin{cases} \geq +1, & \text{class} +1 \\ \leq -1, & \text{class} -1 \end{cases} \tag{8}$$

The two classes are categorized by separation margin (m) given as:

$$m = \frac{2}{\|W\|} \tag{9}$$

In order to maximize m, $\|W\|$ is minimized. The maximum m is obtained by calculating quadratic optimization problem:

$$\min \frac{1}{2}\|W\|^2 \tag{10}$$

subject to $y_i = (W^T x_i + b) \geq 1$.
where $y_i \in \{+1, -1\}$ is the corresponding label for each x_i.

The separation between the classes is maximized by providing the values of W and b. The SVMs are obtained by solving the following dual optimization problem:

$$Max\ L(\alpha) = \sum_{i=1}^{N} \alpha_i - \frac{1}{2} \sum_{i=1}^{N} \sum_{j=1}^{N} \alpha_i \alpha_j y_i y_j x_i x_j \tag{11}$$

subject to $\sum_{j=1}^{N} \alpha_i y_i = 0$ and $\alpha_i \geq 0$.

where α_i is the Lagrangian multiplier and N is the number of training data. The non-linear function Φ is used to obtain a linearly separable data set by mapping the non-linearly separable input space into a higher dimensional feature space. The Kernel function k is utilized to calculate the inner product of input space. Thus, the SVMs are obtained by solving the following optimization problem:

$$Max\ L(\alpha) = \sum_{i=1}^{N} \alpha_i - \frac{1}{2} \sum_{i=1}^{N} \sum_{j=1}^{N} \alpha_i \alpha_j y_i y_j k(x_i, x_j) \tag{12}$$

subject to $\sum_{j=1}^{N} \alpha_i y_i = 0$

where $k(x_i,x_j)$ is the kernel function.

The Gaussian kernel RBF function is given as:

$$k(x_i, x_j) = \exp(-(\|x_i - x_j\|^2) / \gamma) \tag{13}$$

where x_i and x_j are n_dimension input vectors. $\gamma = 2\sigma^2$, σ is the standard deviation of Gaussian. The kernel function parameter (γ) is tuned only once in order to achieve sufficient accuracy [16].

The graphical classification structure is shown in Fig. 4. The procedure of fault analysis in SVM classifier illustrates in Fig. 5. The trained SVM classifiers are tried to find the best class for the features based on (9).

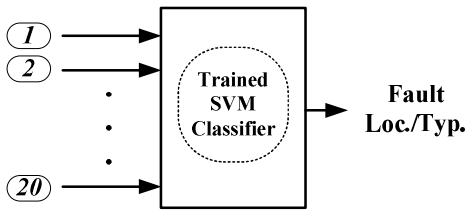

Fig. 4. Classification structure

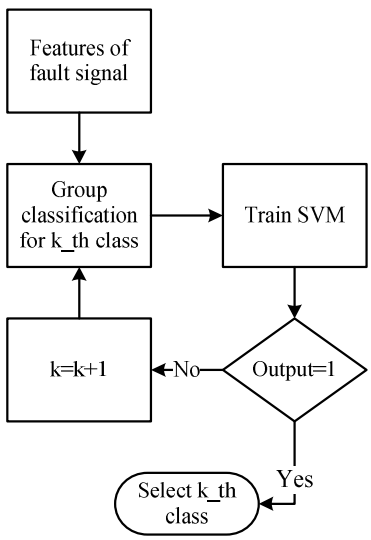

Fig. 5. Procedure of fault analysis in SVM

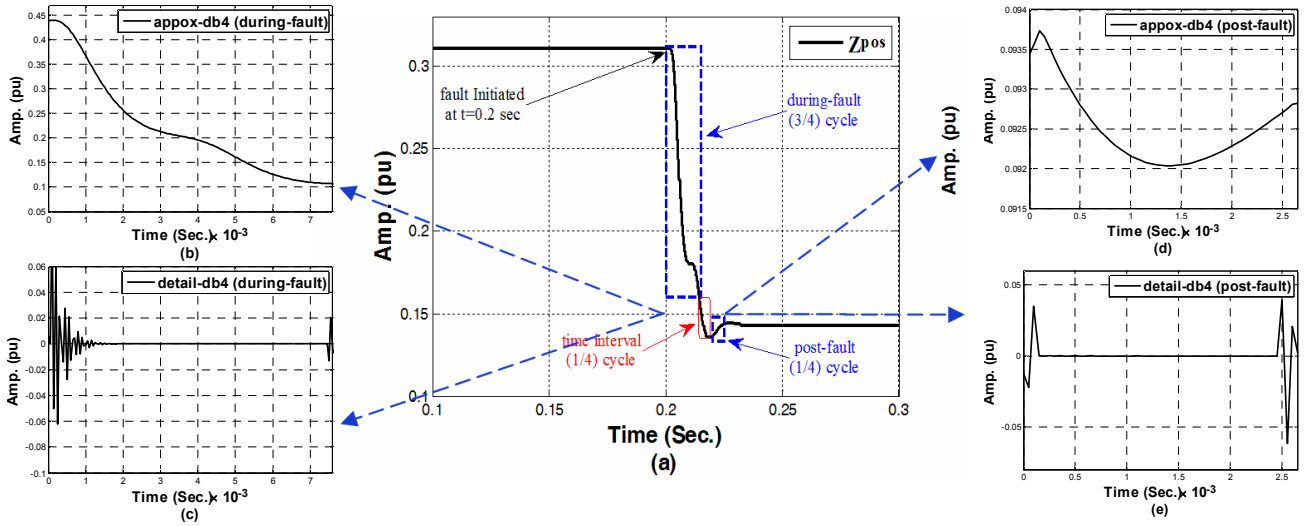

Fig. 6. (a) Fault signal analysis for a solid LLG fault at 33 km with 60° fault angle; (b) Approximation from during-fault; (c) Decomposed detail from during-fault; (d) Approximation from post-fault; (e) Decomposed detail from post-fault

4.2. Feature extraction procedure

Feature extraction algorithm is used to reduce the data analysis complexity, rate of over-fit in algorithms and time of analysis. In this study, the positive sequence impedance is sampled in rate of 11.52 kHz and 20 statistical features are extracted. The faulty portion of the signal is divided into two steps, namely 'during-fault' and 'post-fault' impedance. Fig. 6 (a) represents a fault signal before decomposition. The sub-figure 6 (b) to (e) represent approximation of during-fault, detail of during-fault, approximation of post-fault and detail of post-fault of decomposed signal, respectively. The extracted features are explained as follows:

4.2.1. Average of impedance

The average value ($\bar{x}$) of decomposed fault signal illustrates a meaningful feature. The average of positive sequence impedance on during-fault and post-fault parts are extracted. The average of the impedance is presented in (14). In this equation, 'x_i' represents the i^{th} element of decomposed signal, and 'N' shows the number of sample data in positive sequence impedance.

$$\bar{x} = \frac{1}{N}\sum_{i=1}^{N} x_i \tag{14}$$

4.2.2. Variance of impedance

The next extracted feature from signal is variance (σ^2). This feature provides clearer properties for fault analysis than the average value due to the rate of fluctuation on the decomposed signal.

$$\sigma^2 = \frac{1}{N}\sum_{i=1}^{N}\left(x_i - \bar{x}\right)^2 \tag{15}$$

4.2.3. Weighted arithmetic mean

The weighted arithmetic mean function ($\bar{x}_\omega$) is used to find better discrimination on fault analysis. Implementation of this function highlights the contribution of extrema points which can be more efficient in pattern recognition. The weight of sample 'ω_i' is assigned to represent the sample position in the decomposed signal.

$$\bar{x}_\omega = \frac{\sum_{i=1}^{N}\omega_i x_i}{\sum_{i=1}^{N}\omega_i} \tag{16}$$

4.2.4. Extrema points

The extrema points (minimum and maximum) of each data window range are extracted and compared to find the global maximum and minimum in the selected range.

By using statistical sampling, in total 20 features are extracted. Five features are extracted from approximation of during-fault impedance ($\bar{x}$, σ^2, max, min, $\bar{x}_\omega$) and the same group of features are extracted from detail of during-fault impedance. On the other hand, 10 features are extracted from post-fault impedance in which half of these features are related to approximation and others are related to detail.

4.3. Creating sample data

Four variables in the network are changed to construct different network conditions which are: fault location, fault resistance, fault angle and fault type. Fault type values are selected as integer values which vary from 1-4, representing four categories.

Numbers are assigned for well-known fault types which are listed in Table 2. Fault resistance is selected as a real

Table 2. Fault type classification

Fault Type	LG	LLG	LLLG	LL
Assign No.	1	2	3	4

value. The fault resistance is varied in 12 steps from 0-50Ω [16]. Fault angle is selected as a real value and is varied from 0- 90° in 4 steps. The last output layer for training classifier is fault location.

It is selected as a real value and varied by steps of 1 km in range of 0-100 km over OHL. Moreover, it is varied by steps of 0.2 km in range of 100.01-110 km over UGC. Hence, by changing the fault location, fault resistance, fault type and fault angle, the overall 28992 (151×12×4×4) sample data are created. It is aforementioned that data extraction for a sample data contains 20 features. These features are real values which statistically illustrate the fault signal.

5. Algorithm Evaluation

The classifier is used to estimate the fault location and cluster fault type in the pattern recognition structure. The performance of PM is evaluated based on five different error indices to clearly illustrate the fault analysis method in combined TL. The indicators used h are as follows:

5.1. Mean Square Error (MSE)

This index is routine in classifiers performance evaluation in MATLAB software. MSE presents the risk of a function in the quadratic loss. The mathematical representation of MSE is shown in (17). This index is the summation of the square of difference between the calculated (Y_{cal}) and actual (Y_{act}) values over the number of test data (N).

$$MSE = \frac{1}{N}\sum_{i=1}^{N}\left(Y_{cal} - Y_{act}\right)^2 \tag{17}$$

5.2. Average Error (AE)

This index is a popular one in evaluating the estimation performance. This function is the summation of the difference between calculated and actual values, which is divided by the number of test data. The AE index is represented in (18).

$$AE = \frac{1}{N}\sum_{i=1}^{N}\left(Y_{cal} - Y_{act}\right) \tag{18}$$

5.3. Standard Deviation Error (SDE)

This index calculates the average value of test data error from variance. SDE is the summation of the square of errors divided over the number of test data minus one. The square root of the resultant value presents SDE as follows:

$$SDE = \sqrt{\frac{1}{N-1}\sum_{i=1}^{N}\left(Y_{cal} - Y_{act}\right)^2} \tag{19}$$

5.4. Mean Absolute Percentage Error (MAPE)

This index is well-known in error calculation [23, 25]. The first step of the MAPE calculation is to find the Absolute Percentage Error (APE) for test patterns, as stated in (20):

$$APE = \frac{\left|Y_{cal} - Y_{act}\right|}{Y_{act}} \times 100\% \tag{20}$$

Then, MAPE is calculated by summing APEs as represented in (21). This index represents the error value in percentage.

$$MAPE = \frac{1}{N}\sum_{i=1}^{N} APE_i \tag{21}$$

5.5 Probability Distribution Function (PDF)

The proposed index is widely used in statistical analysis [26]. It is desired to evaluate the classifiers calculated results statistically on normal PDF. This function will illustrate the rate of calculated values with appropriate mother wavelets versus the rate of actual data on a predefined interval. This index represents the error value in percentage.

6. Results and Discussion

The transmission line in Fig. 3 is selected based on [15] to have better comparison and validation with a TW based method. Assume the transmission line total length is 'L'. When a fault occurred in a distance of 'x' from the monitoring bus, the transmission line is divided into three non-homogeneous sections. The first section is from monitoring bus until fault point 'x', the second section is from the fault point to the receiving end bus with the length of 'L–x' and the last section is fault resistance. This perspective can be helpful in simulation to reduce analysis time. The fault point and resistance can be easily changed over TL using this concept. The 'db4' mother wavelet is used to keep decomposed signal resolution in range.

This simulation is done for four well-known fault types. Fault location is changed over TL and fault angle is changed from 0-90°. Finally, fault resistance is changed in a range of 0-50 Ω. For evaluating the proposed

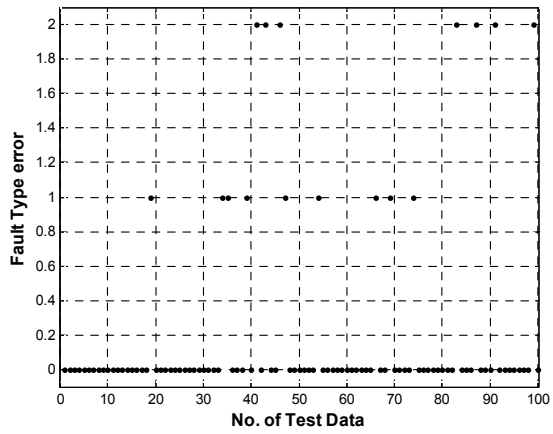

(a)

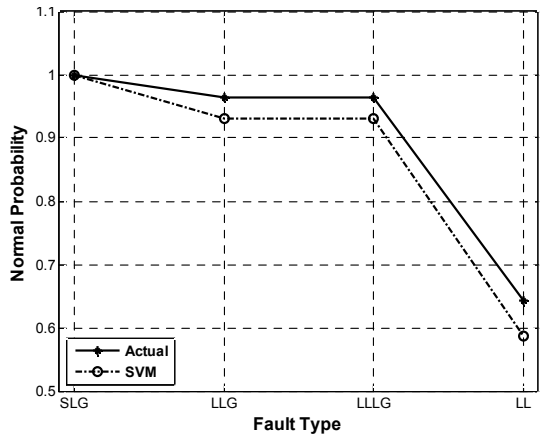

(b)

Fig. 7. (a) Error of fault type clustering of test pattern; (b) PDF of fault type of test pattern

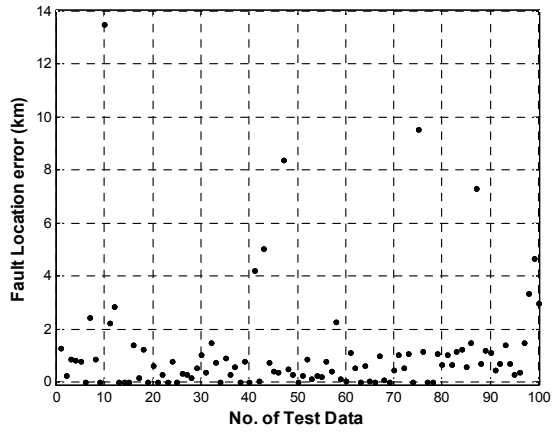

(a)

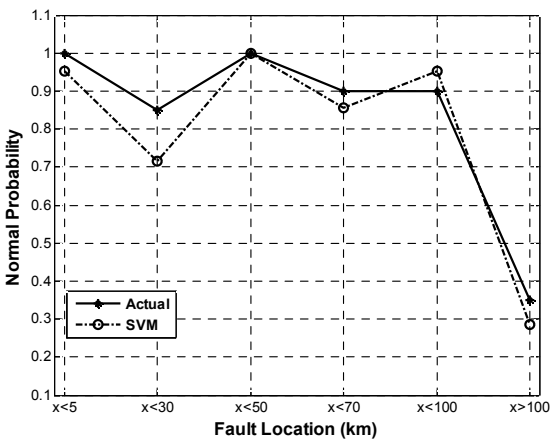

(b)

Fig. 8. (a) Error of fault location estimation of test pattern; (b) PDF of fault location of test pattern

method, overall 100 test patterns are generated by using Monte-Carlo algorithm. The output data are real values of fault type and fault location. Training classifier with a Core-i3 processor and 8 GB of RAM for estimating fault location and clustering fault type took around 12 seconds for SVM.

6.1. Classification of fault type

Fig. 7 (a) proves the ability of proposed sampling method and SVM classifier on clustering the fault type. The error rates are tabulated in Table 3 which shows MSE is 0.37, average error is 0.23 and the standard deviation of errors is 0.566. Moreover, mean absolute percentage error illustrates that the PM has less than 0.1% error while the PDF graph shows a good classification for faults.

Table 3 Error indices for clustering on fault type

Classifier	MSE	AE	SDE	MAPE (%)
SVM	0.37	0.23	0.566	0.0969

6.2. Estimation of fault location

The main target of this study is to find the fault location in combined TL with a significant section of UGC. The fault location estimation by PM always has integer value. This is mainly related to: (*I*) The train data set for fault location is changed by step of 1 km. (*II*) The SVM is a discrete classifier.

Table 4 shows calculated error of the proposed method. The AE of the proposed method is around 1.15 km for the test pattern of Fig. 8 (a). Fig. 8 (b) portrays the good performance of SVM in fault location estimation. The PDF of proposed method is following actual PDF of test pattern. Furthermore, the PM can discriminate between faults on OHL and UGC. This is because of the PDF graphs of actual and PM show close trend. This means that the performance of PM on UGC is fine.

Table 4 Error indices for estimation on fault location

Classifier	MSE (km)	AE (km)	SDE (km)	MAPE (%)
SVM	5.448	1.152	2.05	0.1246

7. Comparison of Proposed Method Ability with Double-ended Travelling Wave Method

The performance of the PM is compared with the existing accurate method in fault detection on combined TL. This TW double-ended technique [15] is used for fault analysis and the proposed network is adequately modeled and sampled. The results and the performance of both methods on fault location estimation and fault type classification are compared and presented. The error is calculated as following [15, 16]:

$$error = \frac{|\,actual\ fault - calculated\ fault\,|}{total\ section\ length} \times 100\% \quad (22)$$

7.1. Fault distance on accuracy of methods

The trained SVM is used to estimate fault distance for LG faults with 10Ω fault resistance. Table 5 presents the evaluation of PM and TW on fault location estimation. The maximum error of TW method in OHL and UGC is not exceeding 0.18% and 1.65%, respectively. On the other hand, the proposed method error by applying SVM classifier in OHL is 1.0% and in UGC is 10%. The PM error is better estimated in OHL compared with UGC. The maximum error of PM is not exceeding 1 km.

7.2. Fault type on accuracy of methods

In this section, the PM and TW methods are tested under faults occurring 30 km away of OHL with fault resistance of 50 Ω and 0° fault angle. The effect of fault type on the accuracy of fault detection in OHL is tabulated in Table 6. TW method accuracy is acceptable except for the ACG fault which increased the ratio to around 0.21% (210 m).

The PM performance is affected by the high resistance and small inception angle in 'LG' fault type. For single line to ground fault the series sequence network increases the fault resistance three times of nominal one [27]. The maximum error for fault location with PM is 2.0% (2 km).

7.3. Fault resistance influence on accuracy of methods

The influence of fault resistance on the accuracy of fault location estimation is presented in Table 7. This table shows a comparison between PM and TW methods for faults at 108 km when fault resistance is varied from 10 Ω to 50 Ω. The maximum error of the TW method did not exceed 1.0% (100 m), but it is close to 10% (1 km) for PM. This is due to double-ended fault location estimation that can increase the accuracy of the TW method.

7.4. Fault angle influence on accuracy of methods

To evaluate fault angle influence on the proposed sampling method, LLG with fault resistance of 10 Ω at fault distance of 90 km on OHL and fault distance of 101 km for UGC with inception angle varied between 0° to 90° in 5 steps. The results are tabulated in Table 8. It is clear that the fault angle impact on fault location estimation of

Table 5. Fault location estimation on PM and TW

	Actual (km)	TW (km)	% error	SVM (km)	% error
OHL	3.5	3.5032	0.0032	4	0.5
	5	5.0048	0.0048	6	1.0
	15	14.9952	0.0048	16	1.0
	20.5	20.6286	0.1286	21	0.5
	40.5	40.6314	0.1314	41	0.5
	50	50.1177	0.1177	50	0.0
	66	66.1174	0.1174	66	0.0
	72	72.1786	0.1786	72	0.0
	83	83.0152	0.0152	83	0.0
	96	95.9880	0.012	97	1.0
UGC	102	102.0192	0.192	103	10.0
	104.2	104.3038	1.038	105	8.0
	106	106.1120	1.12	107	10.0
	107.5	107.6643	1.643	108	5.0
	109.1	109.2325	1.325	110	9.0
	109.5	109.5301	0.301	110	5.0

Table 6. Estimated location with influence of fault type

Actual (km)	TW (km)	% error	SVM (km)	% error
AG	30.0029	0.0029	28	2.0
ACG	30.2094	0.2094	30	0.0
AB	29.9973	0.0027	30	0.0
ABCG	30.0033	0.0033	30	0.0

Table 7. Estimated location with influence of fault resistance

Fault type	Fault resistance	TW (km)	% error	SVM (km)	% error
SLG	10	107.9012	0.9880	109	10.0
SLG	20	107.933	0.6700	109	10.0
SLG	50	107.9875	0.1250	109	10.0
DLG	10	107.902	0.9800	108	0.0
DLG	20	107.9249	0.7510	108	0.0
DLG	50	107.9876	0.1240	109	10.0
TLG	10	107.9327	0.6730	109	10.0
TLG	20	107.9559	0.4410	109	10.0
TLG	50	107.9943	0.0570	108	0.0

Table 8. Estimated location with influence of inception angle

Location	Fault angle	TW (km)	% error	SVM (km)	% error
OHL	0°	89.9908	0.0092	91	1.0
	30°	89.9919	0.0081	91	1.0
	45°	90.0605	0.0605	91	1.0
	60°	89.9997	0.0003	91	1.0
	90°	90.0018	0.0018	91	1.0
UGC	0°	100.8501	1.499	102	10.0
	30°	100.8821	1.179	102	10.0
	45°	101.0579	0.579	102	10.0
	60°	100.9544	0.456	102	10.0
	90°	100.9872	0.128	102	10.0

PM and SVM is constant. The error of PM did not exceed 1 km, but TW method was significantly affected by fault inception angle on UGC section.

8. Comparison of Proposed Method Ability with Single-ended Travelling Wave Method

To have a comprehensive comparison on the fault location estimation, the PM performance is also compared with a single-ended TW method [16]. The critical problem of single-ended TW method for combined transmission line is related to multiple joint-nodes in cable section that cause extensive reflections of high frequency signal. Hence, a technical person with adequate knowledge of TW analysis as well as precision transient recorder are required to find the correct reflected signal. These reasons make single-ended TW fault locator an inaccurate and expensive technique for combined transmission line.

The details of single-ended TW method is represented in Table 9. Although, the PM uses the statistical feature extraction, the single-ended TW utilizes the wavelet transformation coefficients (WTC) for feature extraction. The total sample data for single-ended TW is 2448 which is around one-twelve times of PM. The PM utilizes only one SVM classifier for fault location estimation, but the single-ended TW method uses three SVM classifiers for faulty section identification and fault location calculation. This method required additional calculation based on Bewley lattice diagram for fault location calculation.

The maximum error of fault estimation for PM in case of high resistance (R_f = 50 Ω) is 1.0 km, however it is around 3.22 km for single-ended TW method. In the case of fault with small inception angle ($\alpha \leq 5^{\circ}$), the error is 1.0 km and 3.22 km for PM and single-ended TW method, respectively.

In the case of the worst fault with high resistance simultaneously with small inception angle, the PM error is not exceeding 2.0 km. However, it is around 4.8 km for single-ended TW.

Table 9. The comparison between single-ended methods

Method	PM	TW Single-ended
Mother wavelet	DB-4	DB-4
Modal decomposition	Symmetrical components	Clark decomposition
Extracted feature	Statistical	Wavelet transformation coefficients
Total sample data	28992	2448
No. of SVM	1	3
Kernel function	RBF	RBF
High resistance (R_f= 50 Ω)	1.0 km	3.22 km
Fault inception angle ($\alpha \leq 5^{\circ}$)	1.0 km	3.22 km
Max error in worst case (R_f= 50 Ω and $\alpha \leq 5^{\circ}$)	2.0 km	4.83 km

8. Conclusion

The proposed method is an accurate single-ended method for fault analysis. The performance of using this method over double-ended and single-ended TW based methods are shown by comparing the simulation results. In addition, this PM is an impedance-based approach that is quite cheap compared to the expensive methods of the TW analysis. This method can be applied online or offline according to the power system operator's desire. The PM can be implemented on any power system when it is trained appropriately by sample data. The extracted features by wavelet decomposition on positive sequence impedance are statistically sampled and then used as benchmark for fault analysis. These sample data are used to train SVM to estimate the fault type and fault location. The proposed method can discriminate between faults at OHL and UGC sections.

APPENDIX A

The lumped parameter model does not represent a long transmission line exactly due to non-uniform distributed line parameters. It is possible to find the equivalent circuit of long transmission accompanied by line accuracy. Assume the lumped parameter model is similar to Fig. A1. The series arm of equivalent lumped parameter and the shunt arms are represented by *Z'* and *Y'/2*, respectively. Hence, the normal lumped parameter equation will change to [27]:

$$V_S = \left(\frac{Z'Y'}{2} + 1\right) V_R + Z'I_R \tag{A.1}$$

To obtain the value of equivalent lumped parameter model equal to distributed parameter, the coefficients of V_R and I_R must be identical. The distributed parameter coefficients are as follows:

$$V_S = V_R \cosh \gamma l + I_R Z_c \sinh \gamma l \tag{A.2}$$

Now, equating the coefficient of I_R in equation (A.1) and (A.2):

$$Z' = Z_C \sinh \gamma l \tag{A.3}$$

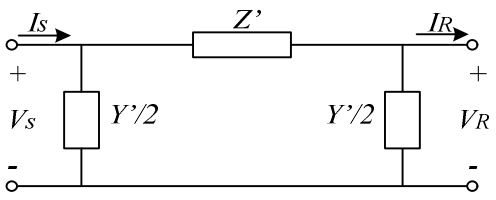

Fig. A1. The equivalent parameter model

$$Z' = \sqrt{\frac{z}{y}} \sinh \gamma l = zl \frac{\sinh \gamma l}{\sqrt{zyl}} \quad \text{(A.4)}$$

$$Z' = Z \frac{\sinh \gamma l}{\gamma l} \quad \text{(A.5)}$$

where Z is equal to zl, the total series impedance of line. The term of $\sinh(\gamma l)/(\gamma l)$ is the factor by which the series impedance of nominal lumped parameter must be multiplied to convert to equivalent lumped parameter.

To investigate the V_R, the coefficient of Eqs. (A.1) and (A.2) is to equate:

$$\frac{Z'Y'}{2} + 1 = \cosh \gamma l \quad \text{(A.6)}$$

By substituting (A.3) and (A.6):

$$\frac{Y'Z_C \sinh \gamma l}{2} + 1 = \cosh \gamma l \quad \text{(A.7)}$$

$$\frac{Y'}{2} = \frac{1}{Z_C} \frac{\cosh \gamma l - 1}{\sinh \gamma l} \quad \text{(A.8)}$$

$$\frac{Y'}{2} = \frac{1}{Z_C} \tanh \frac{\gamma l}{2} \quad \text{(A.9)}$$

$$\frac{Y'}{2} = \frac{Y}{2} \frac{\tanh(\gamma l/2)}{\gamma l/2} \quad \text{(A.10)}$$

where Y is equal to yl, the total shunt admittance of line. The correction factor is used to convert the nominal lumped parameter to equivalent lumped parameter.

Therefore, by substituting (A.3) and (A.10) into equation 6, the finalized equation, taking into account the charging current and non-homogenous TL is represented as the following:

$$\int_{t-T}^{t}\int_{t-T}^{t} V dt^2 = Rl \frac{\sinh \gamma l}{\gamma l} \left[\int_{t-T}^{t}\int_{t-T}^{t} idt^2 - Y/2 \frac{\tanh(\gamma l/2)}{\gamma l/2} \int_{t-T}^{t} V dt \right]_{\gamma l = l\sqrt{\omega CR}}^{L=0} + Ll \left[\int_{t-T}^{t} idt - Y/2 \frac{\tanh(\gamma l/2)}{\gamma l/2} V \right]_{\gamma l = l\omega\sqrt{CL}}^{R=0} \quad \text{(A.11)}$$

APPENDIX B

The test system parameters are listed as the following [15]:

Table B1. Test system parameters

		Pos. & Neg. seq.	Zero seq.
OHL	R (Ω/km)	0.3317	0.4817
	L (mH/km)	1.326	4.595
	C (μF/km)	0.008688	0.004762
UGC	R (Ω/km)	0.024	0.412
	L (mH/km)	0.4278	1.5338
	C (μF/km)	0.2811	0.1529

Voltage: 220 kV and frequency: 50 Hz
Length: OHL 100 km and UGC 10 km
Short circuit level: 500MVA
P_{Load}: 380 MW with PF: 0.8

Acknowledgments

The authors would like to thank Universiti Teknologi Malaysia (UTM) for providing laboratory and supporting for the research and Malaysian Ministry of Higher Education (MOHE) for financial support under FRGS grant (Vote no. 4F911).

References

[1] Sanjari, M. and G. Gharehpetian, "Game-theoretic approach to cooperative control of distributed energy resources in islanded microgrid considering voltage and frequency stability," *Neural computing & applications*, vol.25, no.2, 2014

[2] Sanjari, M.J. and G.B. Gharehpetian, "Unified framework for frequency and voltage control of autonomous microgrids," *IET Generation, Transmission & Distribution*, vol. 7, no. 9, pp.965-972, 2013.

[3] Naderipour, A., Zin, A.A.M., Habibuddin, M.H.B., Miveh, M.R. and Guerrero, J.M., "An improved synchronous reference frame current control strategy for a photo-voltaic grid-connected inverter under unbalanced and nonlinear load conditions," *PloS one*, vol.12, no.2, pp.1-17, 2017.

[4] Lee, J.W., Kim, W.K., Oh, Y.S., Seo, H.C., Jang, W.H., Kim, Y.S., Park, C.W. and Kim, C.H., "Algorithm for fault detection and classification using wavelet singular value decomposition for wide-area protection," *J Electr Eng Technol*, vol. 10, no. 3, pp.729-739, 2015.

[5] Wattanasakpubal, C. and T. Bunyagul, "Algorithm for Detecting, Indentifying, Locating and Experience to Develop the Automate Faults Location in Radial Distribution System," *Journal of Electrical Engineering and Technology*, vol.5, no.1, pp.36-44, 2010.

[6] Livani, H. and C.Y. Evrenosoglu, "A traveling wave based single-ended fault location algorithm using DWT for overhead lines combined with underground cables," *in Power and Energy Society General Meeting*, 2010 IEEE. 2010.

[7] Aguilar, R., F. Pérez, and E. Orduña, "High-speed transmission line protection using principal component analysis, a deterministic algorithm," *IET generation, transmission & distribution*, vol.5, no.7, pp. 712-719, 2011.
[8] Jensen, C.F., *Online location of faults on AC cables in underground transmission systems*, Springer Science & Business Media, 2014.
[9] Zhang, W.H., Rosadi, U., Choi, M.S., Lee, S.J. and Lim, I.H., "A robust fault location algorithm for single line-to-ground fault in double-circuit transmission systems," *Journal of Electrical Engineering and Technology*, vol.6, no.1, pp. 1-7, 2011.
[10] Bayliss, C. and B. Hardy, *Transmission and distribution electrical engineering*, Newnes, 2006.
[11] Yusuff, A., A. Jimoh, and J. Munda, "Fault location in transmission lines based on stationary wavelet transform, determinant function feature and support vector regression," *Electric Power Systems Research*, vol.110, pp.73-83, 2014.
[12] Sadeh, J. and H. Afradi, "A new and accurate fault location algorithm for combined transmission lines using adaptive network-based fuzzy inference system," *Electric Power Systems Research*, vol.79, no.11, pp.1538-1545, 2009.
[13] Alkaran, D.S., Vatani, M.R., Sanjari, M.J., Gharehpetian, G.B. and Yatim, A.H., "Overcurrent relays coordination in interconnected networks using accurate analytical method and based on determination of fault critical point," *IEEE Transactions on Power Delivery*, vol.30, no.2, pp.870-877, 2015.
[14] Gao, B., R. Zhang, and X. Zhang, "A Novel Procedure for Protection Setting in an HVDC System Based on Fault Quantities," *Journal of Electrical Engineering & Technology*, vol.12, no.2, pp.513-521, 2017.
[15] Aziz, M. M. A., D. khalil Ibrahim, and M. Gilany, "Fault location scheme for combined overhead line with underground power cable," *Electric power systems research*, vol.76, no.11, pp.928-935, 2006.
[16] Livani, H. and C.Y. Evrenosoglu, "A machine learning and wavelet-based fault location method for hybrid transmission lines," *IEEE Transactions on Smart Grid*, vol.5, no.1, pp.51-59, 2014.
[17] Gers, J.M. and E.J. Holmes, *Protection of electricity distribution networks*, IET , 2004.
[18] "PCS-996 Disturbance Fault Recorder Instruction Manual". NR Electric Co. Ltd., China, 2014. (www.nrec.com).
[19] "TFS-2100E Travelling Wave Fault Locator System Description and Specification". Istrumentazioni Sistemi Automatici S.r.l., Italy, 2014. (www.isatest.com).
[20] Jung, C.K., Lee, J.B., Wang, X.H. and Song, Y.H., "Wavelet based noise cancellation technique for fault location on underground power cables," *Electric Power Systems Research*, vol.77, no.10, pp.1349-1362, 2007.
[21] Yang, X., Choi, M.S., Lee, S.J., Ten, C.W. and Lim, S.I., "Fault location for underground power cable using distributed parameter approach," *IEEE Transactions on Power Systems*, vol.23, no.4, pp.1809-1816, 2008.
[22] Kase, T., Y. Kurosawa, and H. Amo, "Charging current compensation for distance protection," *IEEE Transactions on power delivery*, vol.23, no.1, pp.124-131, 2008.
[23] Ramesh, B. and P. Arulmozhivarman, "Improving forecast accuracy of wind speed using wavelet transform and neural networks," *Journal of Electrical Engineering and Technology*, vol.8, no.3, pp.559-564, 2013.
[24] Salat, R. and S. Osowski, "Accurate fault location in the power transmission line using support vector machine approach," *IEEE Transactions on power systems*, vol.19, no.2, pp.979-986, 2004.
[25] Shariati, O., Zin, A.M., Khairuddin, A. and Aghamohammadi, "Development and implementation of neural network observers to estimate synchronous generators' dynamic parameters using online operating data," *Electrical Engineering*, vol.96, no.1, 2014.
[26] Sanjari, M., O. Alizadeh Mousavi, and G. Gharehpetian, "Assessing the risk of blackout in the power system including HVDC and FACTS devices," *International Transactions on Electrical Energy Systems*, vol.23, no.1, pp.109-121, 2013.
[27] Grainger, J. J. S., W. D. J. J. Grainger, and W. D. Stevenson, *Power system analysis*, 1994.

Jalal Tavalaei received his B.Sc. in Islamic Azad University, Dezful Branch, (IAUD) Iran and M.Eng. in UTM Malaysia, respectively. He is currently a PhD candidate in Electrical Power Faculty, UTM. His research interests focus on power system monitoring and protection, artificial intelligence and renewable energy.

Mohd Hafiz Habibuddin received B. Eng. (Electrical) (UTM), M. Eng. (Electrical) (UTM) and D. Eng. (Electrical) (Hiroshima) in 2001, 2003 and 2011 respectively. He is a Senior Lecturer in Faculty of Electrical Engineering, Universiti Teknologi Malaysia in Johor, Malaysia. His research interests include power system operation and protection.

Azhar Khairuddin received the B.Sc. degree in electrical engineering from Louisiana State University, U.S.A., and the Master and Ph.D. degrees in electrical engineering from the Universiti Teknologi Malaysia, Johor, Malaysia. He has published many technical papers related to power system locally and internationally. Currently he is an Associate Professor in the Electrical Power Department, Universiti Teknologi Malaysia. His current interests include power system security, deregulation, renewable and distributed generation, and new approaches in teaching for power system courses.

ABDULLAH ASUHAIMI MOHD ZIN (M*88, SM*97) was a Professor at the Faculty of Electrical Engineering, Universiti Teknologi Malaysia (UTM). He received his B.Sc. degree (1976) from Gadjah Mada University, Indonesia, M.Sc. degree (1981) from University of Strathclyde, United Kingdom and Ph.D degree (1988) from UMIST, United Kingdom. He has been teaching at UTM for more than 39 years. He also has authored/co-authored over 190 technical papers. His research interests include power system protection, application of neural network in power system, smart grid, renewable energy, power quality and dynamic equivalent of power system. Dr. Mohd. Zin is also a Corporate Member of The Institution of Engineers, Malaysia (IEM), a Member of IET (UK) and a Senior Member of IEEE (USA). He is a registered Professional Engineer (P. Eng.) in Malaysia and Chartered Engineer (C. Eng.) in United Kingdom.